A Thesis on

"ELECTROCHEMICAL WATER SPLITTING BY REDOX ACTIVE METAL ORGANIC FRAMEWORKS"

Submitted for the partial fulfillment of the requirement for

The award of the degree of the

MASTER OF SCIENCE

In

CHEMISTRY

Submitted By

KOMAL SHARMA

Roll No. 301702018

Under the Supervision of

Dr. RAJ KUMAR DAS

Assistant Professor (Contractual)

School of Chemistry and Biochemistry

Thapar Institute of Engineering and Technology

(Deemed to be University)

Patiala-147004 (Punjab) July 2019

CERTIFICATE

This is to certify that **Ms. KOMAL SHARMA**, Roll No. **301702018** has worked on **"ELECTROCHEMICAL WATER SPLITTING BY REDOX ACTIVE METAL ORGANIC FRAMEWORKS"** dissertation report as a partial fulfillment for the award of the degree of **MASTER OF SCIENCE in CHEMISTRY.** All the information in this dissertation has been presented in accordance with the academic rule and ethical conduct. This is to further state that, no part of dissertation has already been or is being currently submitted to any other University or College in any form for the award of such degree.

Supervisor:

Raj Kumar Das 15/07/2019

Dr. Raj Kumar Das

Assistant Professor (Contractual)

SCBC, TIET

Patiala -147004.

Page | 2

ACKNOWLEDGEMENT

Foremost, I would like to express my deep sense of gratitude and obligations to my worthy supervisor ***Dr. RAJ KUMAR DAS****, for his continuous support in my dissertation. I thank him for him patience, motivation and immense knowledge that carried me through the difficult times and for his insights and suggestions that helped me to shape my research skills. It is a matter of pride and pleasure that I had worked under his generous and able supervision.*

I would like to thank all my honorable Professors of School of Chemistry and Biochemistry, TIET Patiala who have taught me. And I also thanks to ***Dr. Amjad Ali,*** *Professor and Head of Department for providing his support and facilities to conduct this research. I am extremely grateful to* ***Dr. Soumen Basu*** *for sharing his lab facility.*

A special thanks to ***Ms. Surbhi Sharma, Ms. Anchal, Ms. Neeraj and Ms. Divya****, research scholars, for their help and valuable suggestions. I express my sincere thanks to my lab mate* ***Mr. Hemant Kerwal*** *for his valuable support. I am also thankful to all my friends for continuous moral and intellectual support.*

Finally, I must express my very profound gratitude to my parents for providing me with unfailing support and continuous encouragement throughout my years of study. Last but not the least; I thank the Almighty for everything that I am blessed with.

Komal Sharma

Komal Sharma

Roll No.: 301702018

DEDICATED

TO

MY BELOVED FAMILY

(Mr. Jatinder Kumar and Mrs. Sneh Lata)

ABSTRACT

Water splitting has become an important technique in the production of hydrogen that can be used as fuel in various fields. This process requires electrocatalyst with low overpotential and should exhibit best reaction kinetics for HER (Hydrogen Evolution Reaction) and OER (Oxygen Evolution Reaction). In this report we have prepared electrocatalysts with low overpotential for HER and OER. Further XRD, BET studies were done to know the characteristics of prepared catalyst.

CONTENTS

LIST OF TABLES

CHAPTER 1

INTRODUCTION AND LITERATURE REVIEW

1.1 INTRODUCTION

Renewable resources are being explored so to avoid the present energy crisis globally. As these sources produce minimal amount of greenhouse gases thus contributing towards cleaner environment[1]. Power stations use common fossil fuels like coal and oil to generate most of the electricity. During the process a lot of greenhouse gases production takes place, also including carbon dioxide and methane. So, these sources are dirty sources of energy and non-renewable too. Greenhouse gases consequently warming the Earth's atmosphere that is leading to harsh climatic changes, spreading diseases and threatening living things habitat. Due to its high combustion efficiency, non-toxicity and renewable nature, hydrogen is the one of the cleanest and most useful energy material.

Hydrogen and oxygen are two main elements in water, and known to be the most abundant resources on Earth. Hydrogen production can be effectively done through water splitting. Among other schemes for the evolution of hydrogen, water splitting using photocatalyst or electrocatalyst over solar or electrical energy is most promising due to sustainability[2]. The oxygen evolution reaction **(OER)** and the hydrogen evolution reaction **(HER)** are the two half-cell reactions that water splitting is consisted of[3]. However, these reactions need to be catalyzed by various catalysts as they have sluggish kinetics. The two process **OER** and **HER** are catalyzed using precious metal ions (Ir[6], [7]/Ru[4]**,** [5] and Pt[8], /respectively) to achieve the best kinetics. Unfortunately, lower abundance and high cost of noble metals make their use hindered on large scale in electrolysis of water. It is important to look for other catalysts based on precious metals for sustainable hydrogen production with excellent stability and activity. Electrocatalyst composed of non-precious metal (e.g., Co[16], Ni[9]) materials were found to be best alternative to these catalysts for significant activity towards OER and HER. In addition, carbon based materials were found as other options of electrocatalyst for OER and HER. Different forms of carbons (nanotubes[17], graphene[18], etc.) have markedly increased electrocatalysis for OER/HER because of adjustable compositions.

1.2 WATER SPLITTING

The process of water splitting involves decomposition of water into its constituents and enables the production of hydrogen and oxygen. Different energy sources can be used to cleave H-O-H bond like light, heat etc.

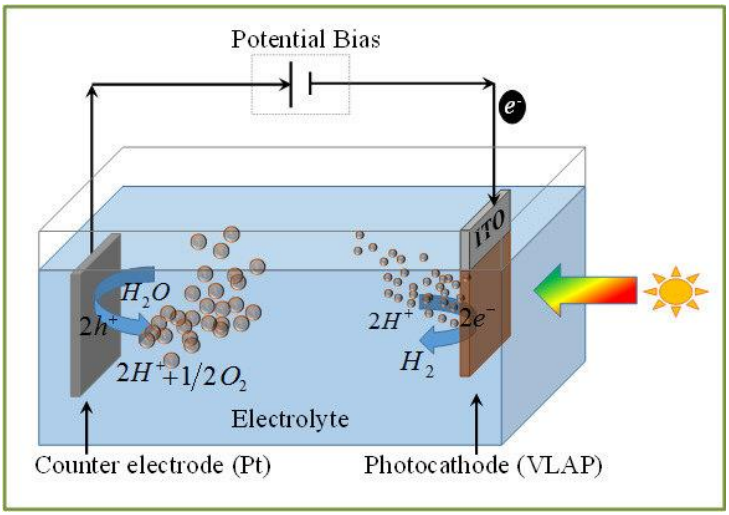

Fig.1. Photocatalytic water splitting with a VLAP photocathode, as a working electrode.

1.2.1 PHOTOCHEMICAL WATER SPLITTING

Photochemical /photocatalytic water splitting involves hydrogen production by splitting of water using sunlight[19]. It is oriented by reduction of CO_2 emission. Water splitting using sunlight is the most important criteria by which redox potential of water can be obtained. In general, conduction bands are formed by empty d or sp orbitals. So for efficient photocatalytic materials, the presence of metal ions having a d^0 and d^{10} electronic configurations are considered to be important (Ta^{5+}, Ti^{4+}, Zr^{4+}, In^{3+}, Sn^{4+}).

1.2.2 THERMOCHEMICAL WATER SPLITTING

Hydrogen evolution is obtained through thermal or thermochemical water splitting involving splitting of water into its elements at (500-2000^{o}C). The process creates cyclic loop converting water into hydrogen and oxygen and reusing the chemicals within each cycle (Fig. 2). This technology is an attractive methodology to produce hydrogen as it uses waste heat.

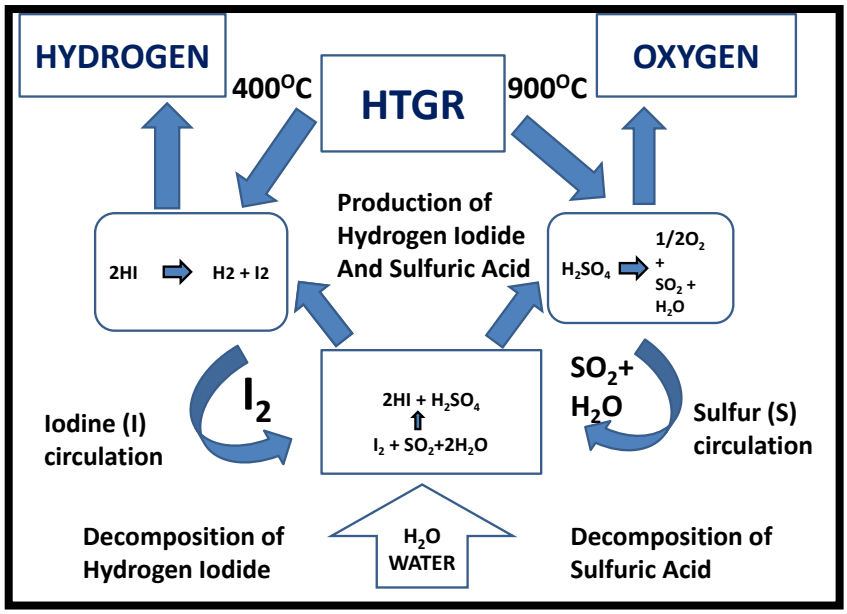

Fig.2. Thermochemical water splitting cycle using iodine and sulfur[24]

1.2.3. ELECTROCHEMICAL WATER SPLITTING

Electrolytic water splitting involves passage of electricity through the water, and electrical energy gets converted to chemical energy via charge transfer reactions at electrode-solution interface called an electrolyser[20]. Hydrogen and oxygen evolution take place at cathode and anode respectively. Due to "zero" CO_2 emission electrolytic water slitting is less environmental harmful including O_2 as the only by-product.

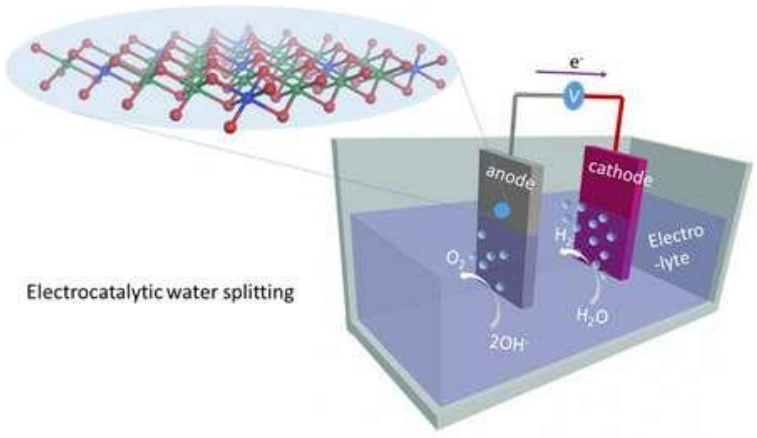

Fig.3. Scheme showing electrochemical water splitting[25]

The reaction for water splitting:

$$2H_2O \rightarrow O_2 + 2H_2 \qquad \textbf{(eq. 1.1)}$$

This process requires energy of 286 kJ mol^{-1} under standard temperature and pressure conditions as it is thermodynamically uphill process. Water splitting has arisen to be the promising method over the last two decades to meet energy demands. So for this purpose firstly to split water, energy is used to drive electrochemical device. Then, the hydrogen produced is stored in a fuel cell and energy demands are met either by burning in air or recombining it with oxygen again. At present commercially available electrolyzers are of two kinds: proton exchange membrane (PEM) and alkaline based electrolyzers. The alkaline electrolyzers achieve specific current densities between 100 and 300 mA cm^{-2} and the former

reach upto 2000 mA cm^{-2}. However, PEM electrolyzers use precious metals as electrode catalysts so they are higher in cost, in contrast with the alkaline electrolyzers that uses Earth abundant elements. Both electrolyzers require materials that can withstand harsh conditions because they both work at extreme pH. Inspite of their outstanding performance PEM and alkaline electrolyzer are not used widely because of costly materials they are made off. Alkaline electrolyzers are cheaper, but a potential leak makes it dangerous to use thus potentially unsafe.

1.3 Water splitting electrochemistry

The overall water splitting reaction consists of following half-reactions:

$2H^+ + 2e^- \rightarrow H_2$ (For HER), with $E_o = 0$ **(eq. 1.2)**

$E = E_o + 0.059 \times 2 \log [H^+]^2 = E_o + 0.059 \log [H^+] = 0\text{-}0.059pH$ **(eq. 1.3)**

$2H_2O \rightarrow O_2 + 4H^+ + 4e^-$ (For OER), with $E_o = 1.23$ **(eq. 1.4)**

$E = E_o + 0.059 \times 4 \log [H^+]^4 = E_o + 0.059 \log [H^+] = 1.23\text{-}0.059pH$ **(eq. 1.5)**

According to above equations voltage difference of only 1.23 V is required between two electrodes to split water. Practically a bigger potential is necessary to apply to overcome kinetic barriers at each electrode and resistances present in cell.

The difference in theoretical and actual potential is called Overpotential (η) needed to split water, and the voltage needed to apply:

$$E_{applied} = 1.23 + \eta_{anode} + \eta_{cathode} + iR \quad \textbf{(eq. 1.6)}$$

By optimizing the cell design, the loss of resistance can be reduced and for activation at each of the electrodes catalysts are added. With changes in pH value potential required to drive half reactions also changes. It do matter while studying the performance of catalyst with potentiostat for one of the two half reactions, whereas it does not matter for an electrolyzer because pH terms cancel each other in overall reaction.

Conversion formula is:

$$E_{RHE} = E + 0.059 \times pH.$$

1.3.1 OVERPOTENTIAL AND ONSET POTENTIAL

The onset potential is the potential at which a reaction starts i.e., current starts to increase and calculated manually. The difference between theoretical and actual potential is called Overpotential (η) which is needed to split water and referred to compare catalysts. The current density chosen is of 10 mA cm^{-2} because it corresponds to 10% of solar power to electricity conversion.

1.3.2 TAFEL SLOPE

The Tafel slope tells about the performance of an electrocatalyst. The current density equation is:

$$j = j_o e\, \alpha F\eta /RT \qquad \textbf{(eq. 1.7)}$$

where j_o = exchange current density, α = transfer coefficient, η = overpotential, F = Faraday constant, R = universal gas constant and T = temperature.

Taking logarithm of eq.1.7

$$\ln j = \ln j_o + \alpha F\eta/RT \qquad \textbf{(eq. 1.8)}$$

Converting eq.1.8 into natural logarithm

$$2.303 \log j = 2.302 \log j_o + 2.303\alpha F\eta/RT \qquad \textbf{(eq. 1.9)}$$

Dividing eq.1.9 by 2.302

$$\log j = \log j_o + \alpha F\eta/2.303RT \qquad \textbf{(eq. 1.10)}$$

This can be arranged as

$\eta = a + b \log j$ **(eq. 1.11)**

a and b are constants and eq.1.11 is called the Tafel equation. If we plot values of logarithm of current density at different values of potential and overpotential a linear region is obtained. This slope shows that how with change in given potential range electrocatalytic catalyst performs. Smaller Tafel slope value means better is the catalyst.

1.3.3 STABILITY

It is important to stabilize the catalyst and for this purpose current density of atleast 10 mA cm^{-2} should be maintained for long time period. And other option is cycling the catalyst multiple times. Instability occurs due to harsh pH conditions where degradation occurs.

1.3.4 FARADAIC EFFICIENCY

The ratio between the actual detected and quantified product, is faradaic efficiency which can be written as

$$\gamma_{Faradaic} = \Delta n^{Effective} / \Delta n^{Faradaic} \quad \textbf{(eq 1.13)}$$

Using Faraday's law:

$$\Delta\eta_{O_2}{}^{\text{Faradaic}} = \frac{\nu_{02}}{\nu_e} \text{FC} = \frac{1\ C}{4\ F} \quad \textbf{for the OER,}$$

$$\Delta\eta_{H_2}{}^{\text{Faradaic}} = \frac{\nu_{H2}}{\nu_e} \text{FC} = \frac{1\ C}{2\ F} \quad \textbf{for the HER,}$$

F is Faraday constant,

where C =charge passed

n= number of moles

ν_e= number of electrons

The Faradaic yield informs if there is some other electrochemical process competing with the reaction under study.

1.3.5 TURNOVER FREQUENCY

Conversion of desired product for catalytic site over time from number of reactants is called turnover frequency. For heterogeneous catalysts, this value is not easy to obtain. It is accessed at only active sites on the surface of catalyst.

1.4 CATALYSTS

1.4.1 PRECIOUS METAL CATALYSTS

Precious metal catalysts have incomplete d-orbitals to donate or withdraw electrons from the reagent, depending upon the nature of the reaction and are also known as 'noble metal catalysts'. So, they show high selectivity and activity in catalysis. They are highly stable thus oxides are difficult to form even on oxidation. They also possess high thermal stability. These kind of catalysts consist of nano-sized precious metal particles highly dispersive in nature supported on materials with large surface area. The adsorption of hydrogen and oxygen present in atmosphere is easy for these nano-scale metal particles. Due to distributive adsorption that occurs through d shell electron of the metal atoms, oxygen and hydrogen becomes highly active. These react with other substituents to give various products under mild conditions.

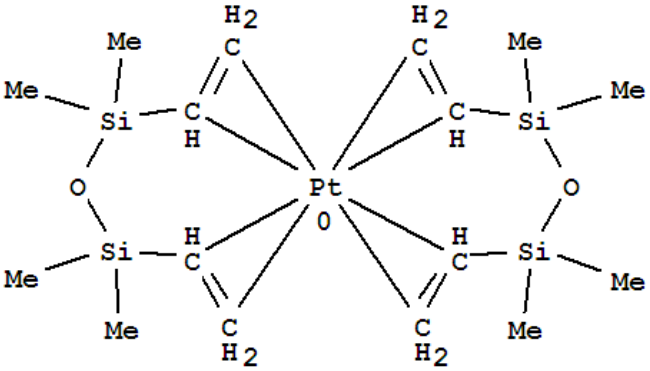

Fig.4. Precious metal based catalyst

Oxides of precious metals are difficult to form due their high stability. Relatively if any oxides are formed they are likely to be very unstable. In acidic or alkaline solution precious metals are not easily dissolvable. For example, for maleic acid hydrogenation, Pd/carbon can be used which is an acidic condition. However, due to leaching for the same reaction Ni catalyst cannot be used. Precious metals have relatively higher melting points than base metals. They are also used as gas purifier because of the high thermal stability. To achieve preferable reaction rate in water splitting a large overpotential is required. To solve this issue excellent precious metal catalysts were developed for HER and OER like Pt and Ru/Ir based catalysts. Due to lower abundance, high cost and lack of stability under electrochemical environment, precious metal catalysts are not suitable for practical applications.

1.4.2 NON PRECIOUS METAL CATALYSTS

Compounds like metal nitrides, metal sulphides, phosphides based on transition metals are of low cost and also possess high activity. So these catalysts are known to be promising catalyst for carrying out OER and HER. These metal catalysts are also a great alternative for IrO2, Pt and Pd based electrocatalyst for water splitting. MoS_2 and MoC_2, the non-precious metal based catalysts perform very well in acid media for HER. Transition metal phosphide (TMPs) which are non-precious has been found as a promising catalyst for both HER and OER. Consequently, asynthesized catalyst NC-NiFeOx@NiFe-P in 1M KOH showed excellent activity for OER and HER. Highly efficient bifunctional catalyst 3D Ni/NiS/N doped mesoporous carbon designated Ni/NiS/NC for water splitting displayed great performance for HER and OER. It was found that OER activity improved for surface oxidized CoP_2 and CoMnP catalysts followed by NiP_2 because of the core shell structure of NiP_2/NiOx.7.

Fig.5. Non-Precious metal (Co) based catalyst[21]

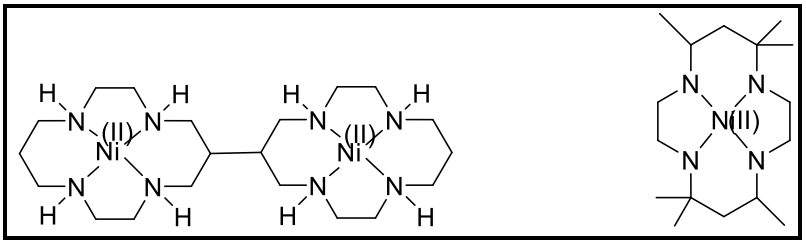

Fig.6. Non-Precious metal (Ni) based catalysts[22], [23]

1.5 MOFs as Electrocatalyst

Nowadays metal-organic frameworks (MOFs) have emerged as new generation catalysts for water splitting due to their remarkable properties such as high surface area, its morphology, and capability to act like precursors, structure and uniform pore channels. Morphology of compound, its hybrids and modifications in structure are the three important designing strategies of MOF based electrocatalyst for water splitting. In electrocatalytic activity morphology plays a vital role for MOFs. For example, electrocatalyst exhibit high electrocatalytic activity with nano octahedrons than nano particles (NPs). In **2011**, Nohra *et al*., reported the direct application of MOFs as catalysts by using MOFs based on polyoxometalate (POMOFs) for HER in electrocatalytic water splitting. Only the structural properties were studied well but it gave very brief information about electrocatalytic activity of POMOFs. Also this gave no idea that how efficient are POMOFs for HER in place of precious metal catalysts. Another POMOF, $[TBA]_3[\varepsilon PMo^{V}_{8}Mo^{VI}_{4}O_{36}(OH)_4Zn_4][BTB]_{4/3}\cdot x$Guest (NENU-500, BTB = benzene tribenzoate, TBA^+ = tetrabutylammonium ion) was reported by Qin *et al*., in **2015** as an ultrastable electrocatalyst for the HER providing an overpotential of 237 mV at a current density of 10 mA cm^{-2} and Tafel slope of 96 mV dec-1, which was inferior to Pt/C. Recently, a MOF was prepared by Dai *et al*. using solvothermal method i.e. MoS_x anchored on Zr-MOF (UiO-66-NH_2) for the HER. Due to large amount of active sites, better electron transfer and favorable protons exchange in Zr-MOFs, HER activity has been enhanced by MoS_x nanosheets. MOFs based on Co were first used by Chaikittisilp and co-workers and that was (zeolitic imidazolate framework-9, ZIF-9). For the potential use in electrocatalysis, Dincă and co-workers developed conductive MOFs. Sun *et al*. obtained isolated Mn_2(DSBDC) exhibiting high charge mobility and great surface area. Sheberla *et al*. in **2014** reported MOFs that were two dimensional made from nitrogen based ligands which are highly conductive. Due to physical durability and high electrical conductivity MOFs are used in electrochemical double layer capacitors (EDLCs). Studies have shown a great increase in the performance of MOFs from past few years. Conductive MOFs are great for electrocatalytic future applications for water splitting as they can be used in supercapacitors as well as fell cells.

CHAPTER 2

RESEARCH GAP AND OBJECTIVES

2.1 RESEARCH GAP

In literature reports, OER and HER were carried out using variety of electrocatalyst. However, in few cases only the structural properties of electrocatalyst were studied providing only brief information related to their electrocatalytic activity (Nohra *et al*., **2011**). For HER an electrocatalyst were prepared with high overpotential and Tafel slope values (Qin *et al*., **2015**). Co-based electrocatalyst were prepared as a precursor for OER which showed overpotential of 410 mA cm^{-2} (Aijaz *et al*.). Although most of the catalyst demand reaction with high overpotential. Even under such conditions also, electrocatalytic activity achieved was not satisfying. Also, the MOFs that act as bifunctional catalyst for both OER and HER are extremely rare. Thus to improve the electrocatalytic activity of electrocatalyst with low overpotential under same reaction conditions for HER and OER, development of new catalyst is essential.

2.2 OBJECTIVES

1) Developing highly active electrocatalyst based on non-precious metals.

2) To prepare high performance redox electrocatalyst with high surface area, charge mobility, high conductivity, more active sites and stability with low overpotential values for HER and OER.

3) To prepare mixed metal organic frameworks (MOFs) as an electrocatalyst by solvothermal method.

4) Characterization of the prepared catalyst by physico-chemical techniques like powder X- ray diffraction (**powder XRD**) and **BET** (Brunauer Emmett Teller).

5) Application of the prepared catalyst for water splitting to produce hydrogen and oxygen.

CHAPTER 3

3 EXPERIMENT METHODS

3.1 MATERIALS

Inorganic salts, Iron(III) chloride ($FeCl_3$), Ferrous chloride ($FeCl_2$), Nickel chloride ($NiCl_2$), Cobalt chloride ($CoCl_2$) and Dimethyl formamide (DMF) from Loba Chemie, Formic acid (HCOOH) from Nice chemicals, Nafion from Sainenergy Fuel Cell India Pvt Ltd, Ethanol (CH_3CH_2OH) from RANKEM and carbon sheet were used directly without any further changes in them.

3.2 METHODS

3.2.1 X-ray Structural Studies

Single crystal X-ray data were collected at 298 K on a Rigaku-Agilent diffractometer using graphite-monochromated MoK_α radiation (λ = 0.71069 Å). The linear absorption coefficients, scattering factors for the atoms, and the anomalous dispersion corrections were taken from International Tables for X-ray Crystallography [10]. The data integration and reduction were processed with SAINT [11] software. An empirical absorption correction was applied to the collected reflections with SADABS [12] using XPREP [13]. The structure was solved by the direct method using SHELXTL [14] and was refined on F^2 by full-matrix least-squares technique using the SHELXL-97 [15] program package. The non-hydrogen atoms were refined anisotropically and the hydrogen atoms are fixed using geometrical constrain (except as noted). The disordered dimethyl ammonium ions have been refined isotropically and its hydrogen atoms cannot be fixed. Data collection, lattice parameters and structure solution parameters are collected in Table 1.

Table 1: Table showing Single Crystal XRD Data

Identification code	solve1
Empirical formula	$C_8Fe_2NO_{12}H_6$
Formula weight	419.84
Temperature/K	298.15
Crystal system	Trigonal
Space group	$P\text{-}3_1c$
a/Å	8.2545(2)
b/Å	8.2545(2)
c/Å	13.8682(3)
α/°	90.00
β/°	90.00
γ/°	120.00
Volume/Å^3	818.34(5)
Z	2
ρ_{calc}g/cm^3	1.704
μ/mm^{-1}	1.829
F(000)	418.0
Crystal size/mm^3	0.24 × 0.18 × 0.15
Radiation	MoKα (λ = 0.71073)
2Θ range for data collection/°	5.7 to 55.96
Index ranges	$-10 \leq h \leq 10$, $-9 \leq k \leq 10$, $-18 \leq l \leq 16$
Reflections collected	3307
Independent reflections	639 [R_{int} = 0.0171, R_{sigma} = 0.0126]
Data/restraints/parameters	639/0/46
Goodness-of-fit on F^2	1.241
Final R indexes [I>=2σ (I)]	R_1 = 0.0288, wR_2 = 0.0827
Final R indexes [all data]	R_1 = 0.0303, wR_2 = 0.0840
Largest diff. peak/hole / e Å^{-3}	0.32/-1.37

3.2.2 Powder X- ray diffraction (XRD)

By using Rigaku Ultima IV fully automatic high resolution X-ray diffractometer system with Theta-Theta (θ-θ) Goniometer, X-ray diffraction patterns of the catalysts synthesized were recorded. With rated tube current of 2-60 mA, the generator operates at 20-60 kV. The samples were scanned in the range of 2Θ=0-90^{o} at the scanning speed of 2 min.

3.2.3 Brunauer Emmett Teller (BET)

The surface area, pore diameter and pore volume of the synthesized MOFs were compared by BET surface area analyzer of autosorb-1, Quanta chrome instruments.

3.3 CATALYST PREPARATION

Mixed valence MOFs were prepared by hydrothermal method for electrocatalytic water splitting.

3.3.1 Preparation of $[(CH_3)_2NH][Fe(III)Fe(II)(HCOO)_6]$(1)

For $[(CH_3)_2NH][Fe(III)Fe(II)(HCOO)_6]$, Iron(III) chloride anhydrous (0.243 g, 1.5 mmol) and Ferrous chloride hydrate (0.190 g, 1.5mmol) was dissolved in DMF (35ml) and Formic acid solution (25ml, 85%) has been taken in a Teflon-lined stainless-steel autoclave. The mixture heated at 140^{O}C for 12 hours under autogeneous pressure. Upon cooling to room temperature it was cooled to obtain extremely dark purple colored crystals. The crystals were washed several times with ethanol and air dried.

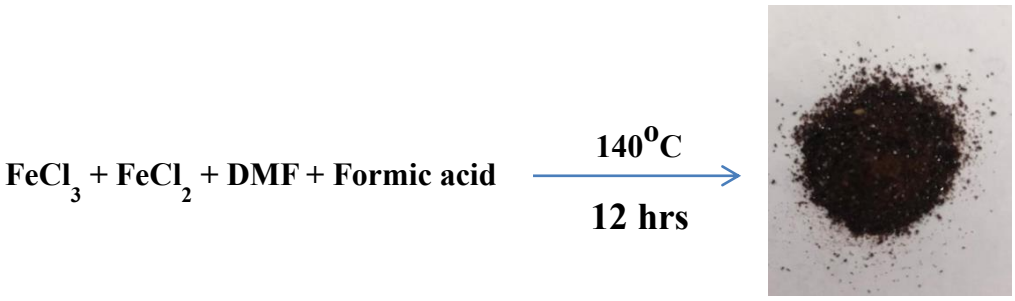

Fig.7 Scheme showing preparation of $[(CH_3)_2NH][Fe(III)Co(II)(HCOO)_6]$

3.3.2 Preparation of $[(CH_3)_2NH][Fe(III)Ni(II)(HCOO)_6]$(2)

For the synthesis of $[(CH_3)_2NH][Fe(III)Ni(II)(HCOO)_6]$, Iron(III) chloride anhydrous (0.243 g, 1.5 mmol) and Nickel chloride hydrate (0.194 g, 1.5mmol) was dissolved in DMF (35ml) and Formic acid solution (25ml, 85%) has been taken in a Teflon-lined stainless-steel autoclave. The mixture heated at $140^{O}C$ for 12 hours under autogeneous pressure. Upon cooling to room temperature.

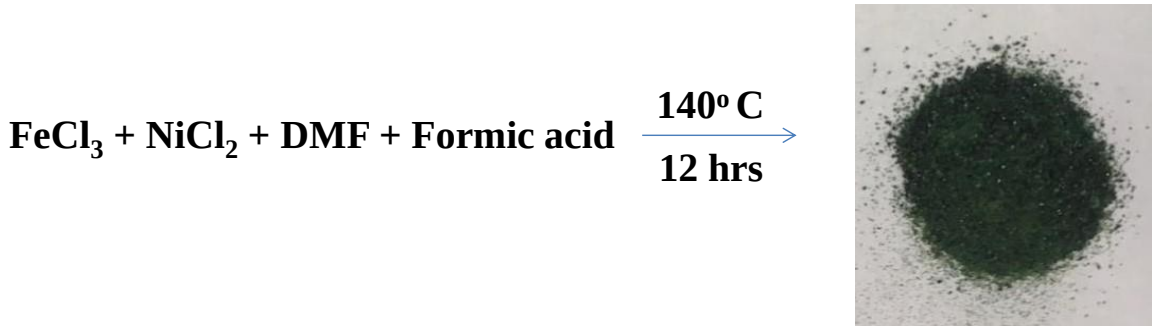

Fig.8 Scheme showing preparation of $[(CH_3)_2NH][Fe(III)Ni(II)(HCOO)_6]$

3.3.3 Preparation of $[(CH_3)_2NH][Fe(III)Co(II)(HCOO)_6]$(3)

To obtain $[(CH_3)_2NH][Fe(III)Co(II)(HCOO)_6]$, Iron(III) chloride anhydrous (0.243 g, 1.5 mmol) and Cobalt chloride (0.194 g, 1.5mmol) was dissolved in DMF (35ml) and Formic acid solution (25ml, 85%) has been taken in a Teflon-lined stainless-steel autoclave. The mixture heated at $140^{O}C$ for 12 hours under autogeneous pressure. Upon cooling to room temperature

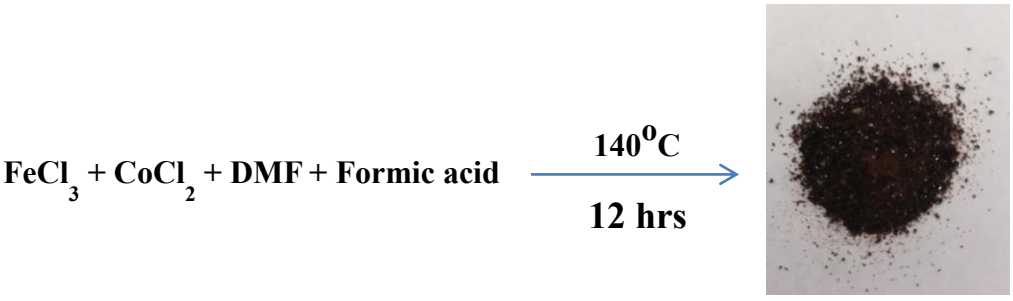

Fig.9 Scheme showing preparation of $[(CH_3)_2NH][Fe(III)Ni(II)(HCOO)_6]$

3.4 WORKING ELECTRODE PREPARATION

For the all working electrodes, crystals of all these MOFs (1 mg) were added to ethanol(5ml) and Nafion(0.1ml) solution in an eppendorf. The mixture was sonicated for 1 hour and the suspension obtained was evenly deposited over 2cm×1cm carbon sheet. It was then oven dried for overnight giving working electrode.

3.5 Preparation of 1M KOH used as an electrolyte

For the preparation of 500ml of 1M KOH, in a volumetric added 28.0582 gm of KOH. After that water was added up to the mark on volumetric. Mixed it well to obtain a clear solution for further electrocatalytic studies.

CHAPTER 4

RESULTS AND DISCUSSION

4.1. SINGLE CRYSTAL XRD ANALYSIS:

This material crystallizes in trigonal *P*-3_1c space group. The asymmetric unit consists of two Fe atoms and a disordered dimethyl ammonium (DMA) group having 1/6 occupancy each, a full occupied formate anion coordinated in an *anti-anti* binding mode (Fig.10).

The bond valence sum (BVS) calculation reveals that Fe1 and Fe2 are having oxidation state +2 and +3 respectively. [17]. The formate anions bridges the metal centers in an to generate the overall three dimensional structure (Fig.11a). The structure consists of alternating layers of Fe(III) and Fe(II) (Fig.11b). The disordered DMA^+ cations occupy the Fe(II) layers (Fig.2b). Individual Fe(II) centers are bridged to six Fe(III) ions in a trigonal prism fashion whereas each Fe(III) is surrounded by six Fe(II) in an octahedral arrangement (Fig. 12).

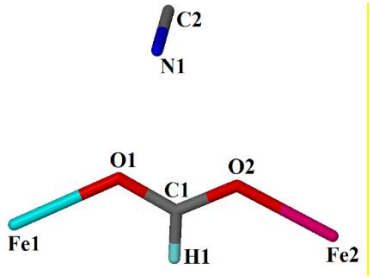

Fig.10. View of Assymmetric Unit in **1**.

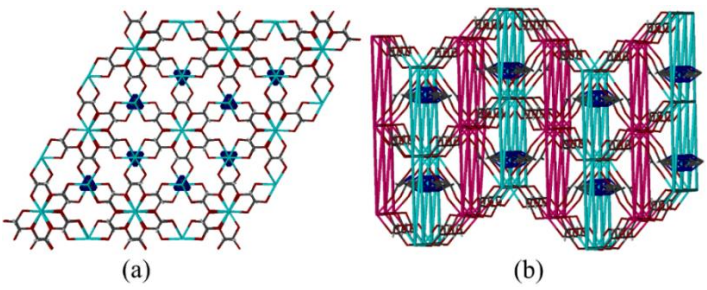

Fig.11 Perspective View of **1** showing (a) Packing along crystallographic c axis (b) Alternative layers of Fe(III) and Fe(II) with embedded dimethyl ammonium cation.

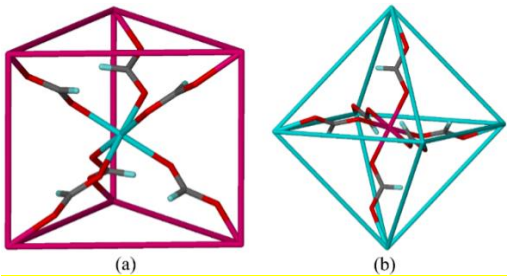

Figure 12. Perspective View of **1** showing (a) Trigonal Prismatic arrangement of Fe(III) around Fe(II) centers and (b) Octahedral arrangement of Fe(II) around Fe(III) centers.

4.2 XRD Analysis

The powder XRD studies have been performed for the prepared mixed valence MOFs $[(CH_3)_2NH][Fe(III)Fe(II)(HCOO)_6]$ (**1**), $[(CH_3)_2NH][Fe(III)Ni(II)(HCOO)_6]$ (**2**), $[(CH_3)_2NH][Fe(III)Co(II)(HCOO)_6]$ (**3**). Their diffraction patterns were compared and are shown in **Fig.13**. It suggests that all the three catalyst exhibits similar kind of diffraction patterns. It is observed that diffraction pattern of the three catalysts **1**, **2** and **3** corresponds to that of simulated.

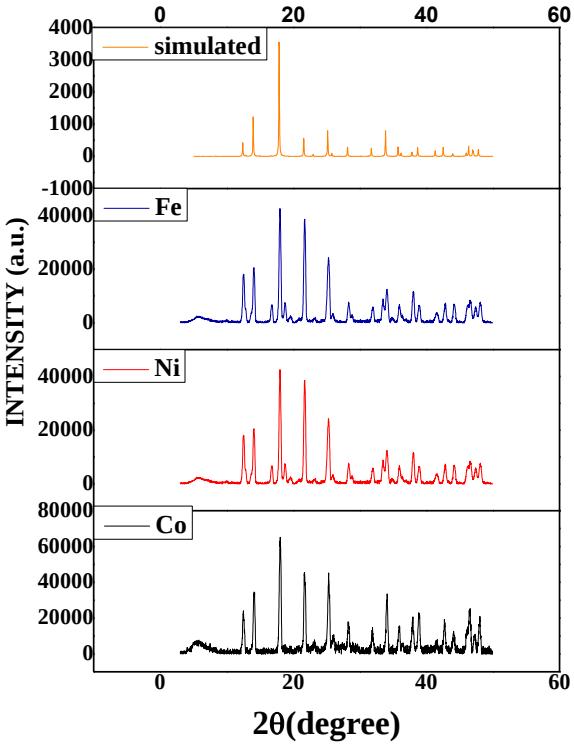

Fig.13. XRD Diffraction Pattern of **1**, **2** and **3**

4.3 BET SURFACE AREA ANALYSIS

Surface area of the as prepared catalyst **1**, **2** and **3** were analyzed by using BET. In this analysis N_2 desorption-adsorption was performed to determine the surface area of prepared catalysts. Initially samples were preheated in a vacuum oven at 100^{o}C for about 5-6 hours to eliminate any kind of additional foreign particle before N_2 adsorption/desorption.

The isotherms are supposed to be prevented from any other adsorbents on the surface. The specific surface area of **1**, **2** and **3** were calculated ~0.23 m^2/g, ~22.9 m^2/g and ~17.1 m^2/g respectively. The pore size distribution of prepared catalysts was obtained by using BJH method. The total pore volume obtained for catalyst **3** is ~0.0034 cm^3/g and the corresponding mean pore diameter is 7.9638 nm. For catalyst **1** the pore volume calculated is ~0.00 cm^3/g and the corresponding mean pore diameter is ~0.00 nm. For catalyst **2** the pore volume is ~0.00488 cm^3/g and the corresponding mean pore diameter obtained is 8.5162 nm.

Fig.14a shows N_2 adsorption and desorption isotherms of **1**, **2** and **3** suggesting the mesoporous nature of prepared catalysts corresponding to IV adsorption isotherm. **Fig.14b** shows pore size distribution of **1**, **2** and **3**. It is observed that all the three catalyst exhibits similar kind of pattern and most of the peak lies between 2-5 nm which suggests the mesoporous nature of **1**, **2** and **3** catalyst.

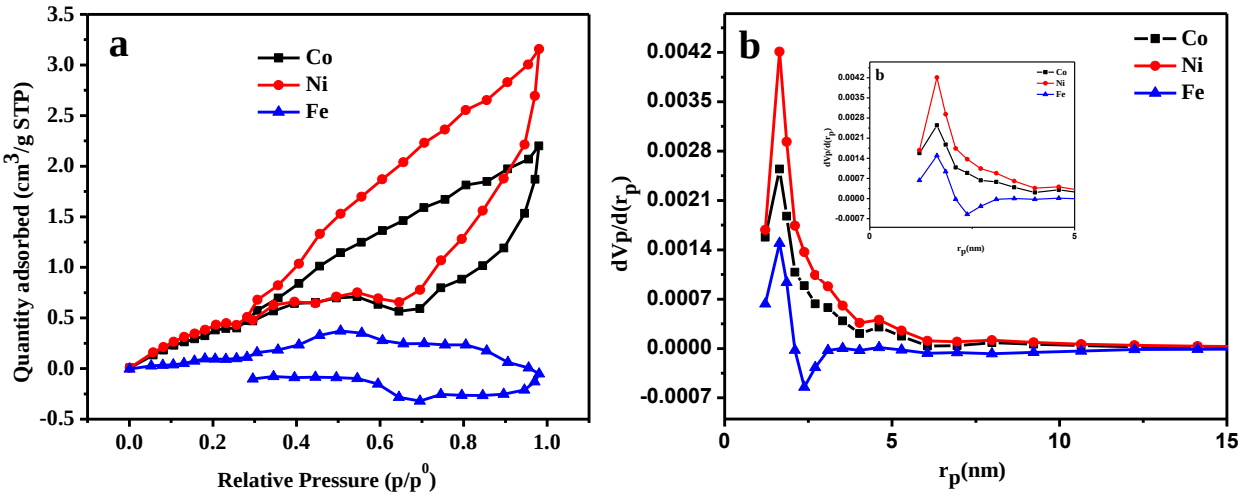

Fig.14. (a) N_2 adsorption and desorption isotherms of as prepared Co, Ni, Fe-based catalysts and (b) pore size distribution of prepared Co, Ni, Fe-based catalysts.

Table.2. Comparison of $[(CH_3)_2NH][Fe(III)Co(II)(HCOO)_6]$, $[(CH_3)_2NH][Fe(III)Co(II)(HCOO)_6]$, $[(CH_3)_2NH][Fe(III)Co(II)(HCOO)_6]$ through BET Surface Area Analyzer.

CATALYST	Surface Area (m^2g^{-1})	Pore Diameter (nm)	Pore Volume (cm^3g^{-1})
$[(CH_3)_2NH][Fe(III)Co(II)(HCOO)_6]$	17.1	7.9638	0.0034
$[(CH_3)_2NH][Fe(III)Ni(II)(HCOO)_6]$	22.9	8.5162	0.00488
$[(CH_3)_2NH][Fe(III)Fe(II)(HCOO)_6]$	0.23	0.00	0.00

4.4 ELECTROCHEMICAL ANALYSIS

4.4.1 OER ANALYSIS

By recording the linear sweep voltammetry (**LSV**) polarization curves, electrocatalytic activity of as prepared catalyst were evaluated for OER (Oxygen evaluation reaction) using a three electrode system having Ag/AgCl/KCl as reference electrode, the MOFs as working electrodes, and Pt as counter electrode using 1M KOH solution as the electrolyte with a scan rate of 10 mVs^{-1}. Fig.1a shows the LSV polarization curves comparing the **3**, **2** and **1**. These MOFS require overpotential values of 403, 461 and 442 mV respectively **(Fig. 15a)**. Thus, it suggests that catalyst **3** exhibits superior activity followed by **2** and **1**.

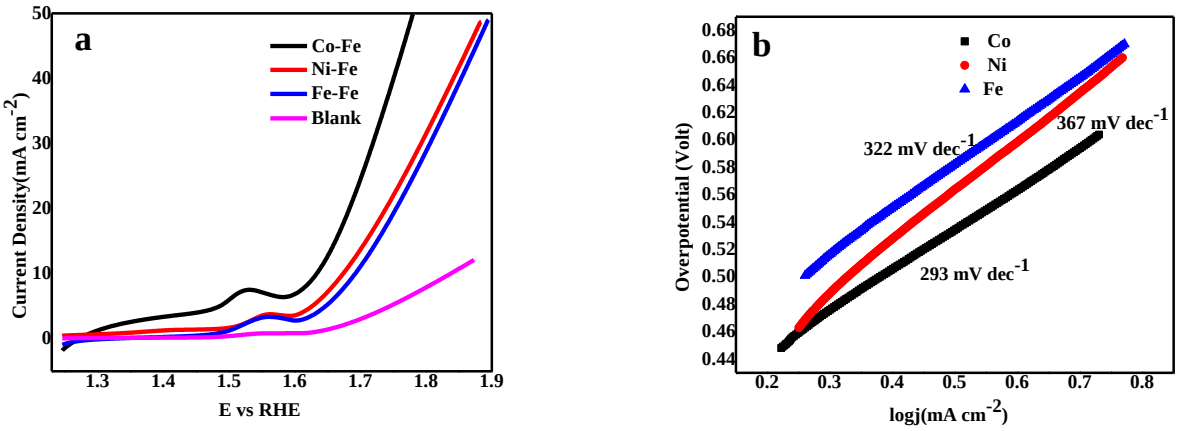

Fig.15.(a) The polarization curves for OER and (b) the relate Tafel plots of Co/Fe, Ni/Fe, Fe/Fe-based catalyst in 1.0 M KOH

.

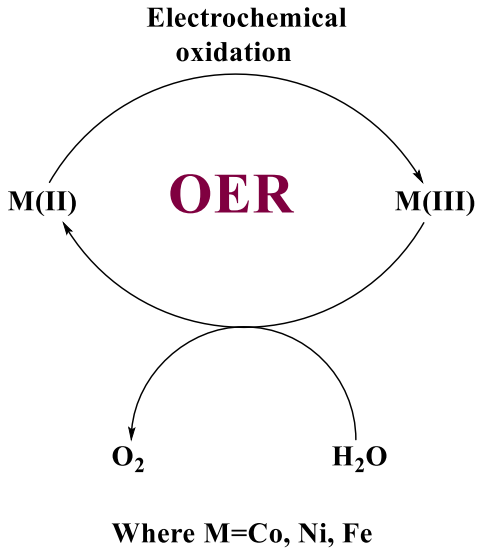

Fig.16. Scheme showing mechanism for OER

Based on these observations we suggest the following mechanism for OER. First the divalent cation undergoes oxidation to its trivalent state followed by oxidation of water by the trivalent cation.

Now in case of Ni it is more difficult to oxidize to Ni(III) so the first step is slow where in case Fe it gets oxidized to Fe(III) very easily but its reduction to Fe(II) is comparatively less favored. In case Co both these steps occurs at optimum rate compared to other two. Such assumptions are validated by the OER activities of these MOFS. The related Tafel plots are shown in Fig.2.b and from the Tafel equation, yielding Tafel slopes of 293, 322, 367 mV dec^{-1} for **3**, **2**, **1** respectively. The Tafel slope values suggest that **3** catalyst exhibits the best OER kinetics.

4.4.2 HER ANALYSIS

The electrocatalytic hydrogen evaluation reaction (**HER**) activities of these as prepared mixed MOFs were evaluated by recording the linear sweep voltammetry (**LSV**) polarization curves using a three electrode system having Ag/AgCl/KCl as reference electrode, the MOFs as working electrodes, and Pt as counter electrode using 1M KOH solution as the electrolyte with a scan rate of 10 mVs^{-1}. **Fig.17a** shows the LSV polarization curves comparing the **1**, **2** and **3**. These MOFS require overpotential values of 196, 229 and

213 mV respectively (**Fig. 17a**). Thus, it suggests that catalyst **1** exhibits superior activity followed by **2** and **3**.

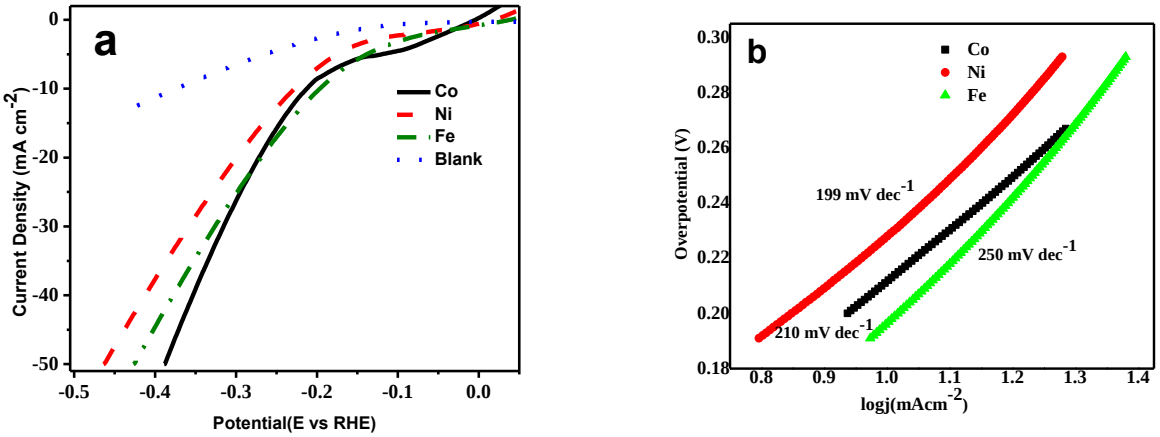

Fig.17.(a) The polarization curves for HER and (b) the related, Tafel plots of Co/Fe, Ni/Fe, and Fe/Fe-based catalyst in 1.0 M KOH.

Based on these observations we suggest the following mechanism for HER. First the trivalent cation undergoes reduction to its divalent state followed by reduction of water by the divalent cation **(Fig 18).**

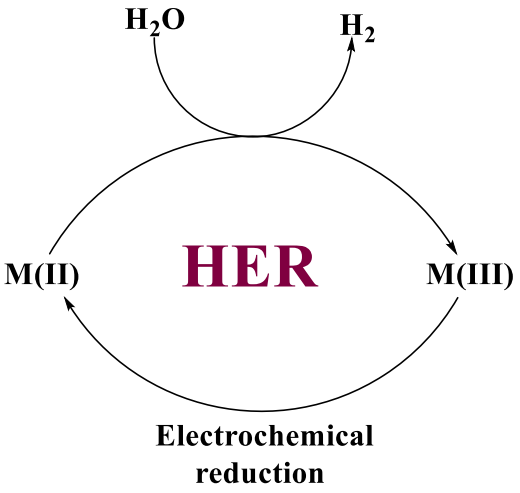

Where M=Co, Ni, Fe

Fig.18. Scheme showing mechanism for HER.

Among all three divalent ions Fe(II) is the strongest reducing agent as a result the Fe-base catalyst shows lowest overpotential for **HER**.. Such assumptions are validated by the HER activities of these MOFS. The related Tafel plots are shown in **Fig.17.b** and from the Tafel equation, yielding Tafel slopes of 199, 210, 250 mV dec^{-1} for **1**, **2**, **3** respectively. The Tafel slope values suggest that **1** catalyst exhibits the best **HER** kinetics.

4.4.3 OVERALL WATER SPLITTING ANALYSIS

Inspired by all the above electrochemical studies, we studied the performance of catalyst **1**, **2**, **3** for water splitting in 1 M KOH. **Fig.19.(a)** shows water splitting polarization curve for the three catalyst **1**, **2**, **3**. The curve suggests that for catalyst **1** the potential achieved is 1.99 V. For catalyst **2** the potential obtained is 1.98 V and for catalyst **3** the obtained potential is 1.93 V. From the data it can be observed that catalyst **3** gives smaller potential value compared to **2** and **1** at same current density.

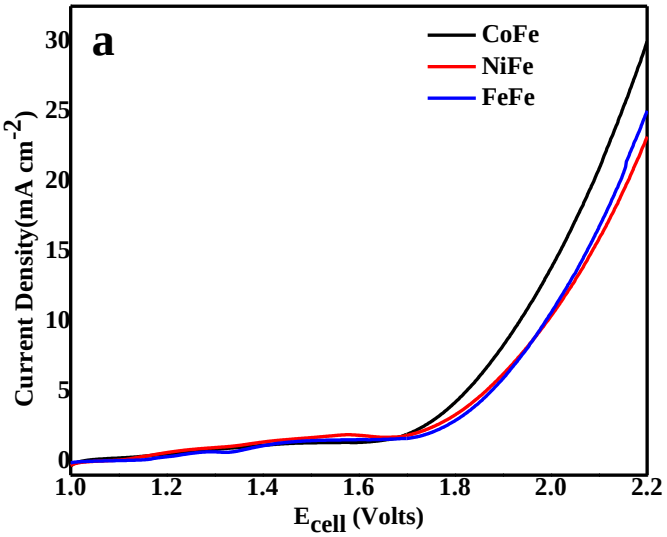

Fig.19.(a) Linear Sweep Voltammetric curves of water splitting of the three prepared catalyst 1, **2**, **3**.

CHAPTER 5

CONCLUSION AND FUTURE SCOPE

Among the three prepared catalysts it is found that catalyst **1 and 3** exhibit excellent electrocatalytic performance for both HER and OER respectively. With low overpotential values of 192 mV and 403 mV for HER and OER respectively, clearly determines that catalyst based on Fe and Co are best for water splitting reactions. Water splitting plays an important role in fuel generation. With the process of water splitting a lot of hydrogen production takes place that can be stored as fuel for various purposes. With great electrocatalyst exhibiting great activity enhances water splitting reaction. Thus this field has great future scope. Although we studied the activity of prepared catalyst but stability and Faradaic efficiencies of prepared catalysts has to further studied.

REFERENCES

1. N. S. Lewis and D. G. Nocera, *Proc. Natl. Acad. Sci. U. S. A.*, 2006, **103**, 15729.
2. J. O. M. Bockris, *Int. J. Hydrogen Energy*, 2002, **27**, 731–740.
3. D. Merki and X. Hu, *Energy Environ. Sci*., 2011, **4**, 3878–3888.
4. S. Neudeck, S. Maji, I. López, S. Meyer, F. Meyer and A. Llobet, *J. Am. Chem. Soc*., 2014, **136**, 24 –27.
5. E. Tsuji, A. Imanishi, K.-I. Fukui and Y. Nakato, *Electrochim. Acta*, 2011, **56**, 2009–2016.
6. R. Lalrempuia, N. D. McDaniel, H. Müller-Bunz, S. Bernhard and M. Albrecht, *Angew. Chem., Int. Ed*., 2010, **49**, 9765–9768.
7. S. W. Sheehan, J. M. Thomsen, U. Hintermair, R. H. Crabtree, G. W. Brudvig and C. A. Schmuttenmaer, *Nat. Commun*., 2015, **6**, 6469.
8. A. Mills, *Chem. Soc. Rev*., 1989, **18**, 285–316.
9. Y F. Evangelisti, R. Güttinger, R. Moré, S. Luber and G. R. Patzke, *J. Am. Chem. Soc*., 2013, **135**, 18734–18737.
10. 3+
11. D. C. Creagh and W. J. McAuley, International Tables for Crystallography, ed. A. J. C. Wilson, Kluwer Academic, Boston, 1992.
12. SAINT+, 6.02ed.; Bruker AXS, Madison, WI, 1999.
13. G. M. Sheldrick, SADABS, Empirical Absorption Correction Program, University of Göttingen, Germany, 1997.
14. XPREP, 5.1 ed. Siemens Industrial Automation Inc., Madison, WI, 1995.
15. G. M. Sheldrick, SHELXTL ™ Reference Manual: version 5.1, Bruker AXS, Madison, WI, 1997.

16. G. M. Sheldrick, SHELXL-97, Program for Crystal Structure Refinement, University of Göttingen, Göttingen, Germany. 1997.
17. Han, Y. Wu, W. Lai and R. Cao, *Inorg. Chem*., 2015, **54**, 5604–5613.
18. X. Hu and S. Dong, *J. Mater. Chem.*, 2008, **18**, 1279–1295.
19. J. Xiao, Q. Kuang, S. Yang, F. Xiao, S. Wang and L. Guo, *Sci. Rep*., 2013, **3**, 2300.
20. S. Kaufhold, L. Petermann, R. Staehle and S. Rau, *Coord. Chem. Rev*., 2015, 304–305, **73 –87**.
21. J. Wang, *Analytical Electrochemistry*, John Wiley & Sons, New Jersey, 2006.
22. J. I. Goldsmith, W. R. Brunschwig, J.R. Winkler and H. B. Gray, *Acc. Chem. Res*., 2009, **42**, 1995-2004.
23. B. J. Fisher and R. Eisenberg, *J. Am. Chem. Soc*., 1980, **102**, 7361-7364.
24. J. P. Collin, A. Jouaiti and J. P. Sauvage, *Inorg. Chem*., 1988, **27**, 1986-1990.
25. K. Onuki, S. Kubo, A. Terada, N. Sakaba and R. Hino, *Energy Environ. Sci*., 2009, **2**, 491-497.
26. K. Fan, H. Chen, Y. Ji, H. Huang, P. M. Claesson, *Nature Comm*., 2016, **17.**

Komal Thesis

ORIGINALITY REPORT

13%	8%	8%	4%
SIMILARITY INDEX	INTERNET SOURCES	PUBLICATIONS	STUDENT PAPERS

PRIMARY SOURCES

1	theses.gla.ac.uk Internet Source	2%
2	Bo Xu, He Yang, Lincheng Yuan, Yiqiang Sun, Zhiming Chen, Cuncheng Li. "Direct selenylation of mixed Ni/Fe metal-organic frameworks to NiFe-Se/C nanorods for overall water splitting", Journal of Power Sources, 2017 Publication	2%
3	onlinelibrary.wiley.com Internet Source	2%
4	Zhao, Jiong-Peng, Bo-Wen Hu, Francesc Lloret, Jun Tao, Qian Yang, Xiao-Feng Zhang, and Xian-He Bu. "Magnetic Behavior Control in Niccolite Structural Metal Formate Frameworks $[NH_2(CH_3)_2][Fe^{III}M^{II}(HCOO)_6]$ (M = Fe, Mn, and Co) by Varying the Divalent Metal Ions", Inorganic Chemistry, 2010. Publication	1%

Iwatsuki, Jin, Shinji Kubo, Seiji Kasahara,

Raj Kumar Das

15/07/19